

## A Monte Carlo model for estimating tornado impacts

Stephen M. Strader,\* Thomas J. Pingel and Walker S. Ashley

*Meteorology Program, Department of Geography, Northern Illinois University, DeKalb, IL, USA*

**ABSTRACT:** Determining the likelihood and severity of tornado disasters requires an understanding of the dynamic relationship between tornado risk and vulnerability. As population increases in the future, it is likely that tornado disaster frequency and magnitude will amplify. This study presents the Tornado Impact Monte Carlo (TorMC) model, which simulates tornado events atop a user-defined spatial domain to estimate the possible impact on people, the built-environment or other potentially vulnerable assets. Using a Monte Carlo approach, the model employs a variety of sampling techniques on observed tornado data to provide greater insight into the tornado disaster potential for a location. Simulations based on 10 000 years of significant tornado events for the relatively high-risk states of Alabama, Illinois and Oklahoma are conducted to demonstrate the model processes, and its reliability and applicability. These simulations are combined with a fine-scale (100 m), residential built-environment cost surface to illustrate the probability of housing unit impact thresholds for a contemporary year. Sample results demonstrate the ability of the model to depict successfully tornado risk, residential built-environment exposure and the probability of disaster. Additional outcomes emphasize the importance of developing versatile tools that capture better the tornado risk and vulnerability attributes in order to provide precise estimates of disaster potential. Such tools can provide emergency managers, planners, insurers and decision makers a means to advance mitigation, resilience and sustainability strategies.

**KEY WORDS** tornado; Monte Carlo; impacts; exposure; risk; disaster

*Received 11 September 2015; Revised 3 December 2015; Accepted 11 December 2015*

### 1. Introduction

Over the last 80 years, the frequency and magnitude of weather-related disasters and losses have been increasing (Bouwer, 2011; Smith and Katz, 2013). The attribution of the underlying cause for the observed amplification in weather-related disaster frequency and magnitude is a contentious topic (Pielke, 2005; Bouwer, 2011; Huggel *et al.*, 2013; Kunkel *et al.*, 2013). However, at the most fundamental level it involves the juxtaposition of a hazard event (e.g. risk of a tornado) with people and their assets (e.g. vulnerability of a certain segment of the populace, housing, critical infrastructure, to a tornado) that determines disaster potential, consequence and severity. To date, there has been limited research determining how risk and vulnerability interact to shape tornado disaster characteristics. Even less attention has been paid to developing tools and methodologies to examine the dynamic relationship between tornado risk and vulnerability.

In the present research, tornado risk is defined as the spatiotemporal probability of tornado occurrence, or hazard, of a certain magnitude, whereas tornado vulnerability is represented by a basic physical exposure metric (e.g. the number of individuals, households or some other tangible asset potentially affected by a tornado). While vulnerability includes other components – such as adaptive capacity (i.e. coping, or adapting, to a hazard) and sensitivity (i.e. degree to which a system is impacted by a hazard), these components and their interactions are often very

complex and difficult to quantify at a high resolution across a large spatiotemporal domain (Cutter *et al.*, 2009; Morss *et al.*, 2011). For this reason, this study focuses on a quantifiable and well-measured variable, the housing unit (HU), to exemplify aspects and utility of the model.

The initial goal of this research is to present a tool that examines the interaction of tornado risk and vulnerability to measure tornado disaster frequency, magnitude and disaster potential better, whether from a historical or future perspective. The described Tornado Impact Monte Carlo (TorMC) model simulates years of tornado events atop a geographical region while assessing their impacts, or costs, on the underlying physical vulnerability landscape. To demonstrate the utility and efficacy of the TorMC model, 10 000 years of significant ( $\geq$  Enhanced Fujita Scale 2 magnitude or EF2+) tornadoes were simulated for the states of Alabama, Illinois and Oklahoma to estimate the number of HUs affected by each path in an hypothetical contemporary year. Simulation results as well as model sensitivity and reliability are highlighted through a number of statistical and graphical procedures.

### 2. Background

As populations continue to grow, the increased placement of people and their assets in physically vulnerable locations is leading to greater disaster potential (Changnon *et al.*, 2000; Nicholls and Small, 2002; Burkett and Davidson, 2012; Ashley *et al.*, 2014; Ashley and Strader, 2015; Strader and Ashley, 2015). Recent studies have sought to examine tornado risk and vulnerability (namely, the exposure component) by using geographic information systems (GIS). Over the last decade, advancements in GIS capabilities and affiliated datasets have permitted studies to

\* Correspondence: S. M. Strader, Meteorology Program, Department of Geography, Northern Illinois University, Davis Hall, Rm. 118, DeKalb, IL 60115, USA. E-mail: sstrader@niu.edu

superimpose tornado events or their likeness atop exposure landscapes to analyse potential tornado impacts and losses on populations (Rae and Stefkovich, 2000; Wurman *et al.*, 2007; Ashley *et al.*, 2014; Rosencrants and Ashley, 2015). Recent research has also coupled Monte Carlo (MC) simulation methods with the tornado hazard to provide greater insight into tornado incidence (Meyer *et al.*, 2002) and impacts on policyholders (Daneshvaran and Morden, 2007). MC simulation is a computational modelling technique that employs repeated random sampling to obtain the distribution of an unknown probabilistic entity (Mooney, 1997). This technique is distinguished from other types of computational models because of two unique characteristics, iteration and randomness. The ability of MC simulations to provide probabilistic rather than deterministic solutions yields greater value to stakeholders and those with a vested interest as it provides more information about likely ‘best case’ and ‘worst case’ outcomes.

In the last 2 decades, MC simulations were employed in the field of hazard sciences to examine the effects and consequences of relatively rare, yet high-impact, geophysical events (Meyer *et al.*, 2002; Rahman *et al.*, 2002; Apel *et al.*, 2004; Daneshvaran and Morden, 2007). In the hazards research community, MC simulations have often been employed to acquire probability distributions (Meyer *et al.*, 2002), return intervals or periods (Rahman *et al.*, 2002; Daneshvaran and Morden, 2007) and/or probability of exceedence (POE) measures of extreme events (Apel *et al.*, 2004). More recently, models employing MC simulation techniques were developed in the reinsurance and catastrophe modelling fields (e.g. Aon Impact Forecasting, Swiss Re, Gen Re). However, most of these models are proprietary and unavailable to researchers. To date, only two available studies (Meyer *et al.*, 2002; Daneshvaran and Morden, 2007) have applied MC simulation techniques to the tornado hazard. The MC simulation in a study by Meyer *et al.* (2002) used random sampling from statistical distributions of tornado characteristics (i.e. occurrence, number of tornadoes, path length and width, magnitude) to model solely significant tornado occurrence in the conterminous United States. In the study by Daneshvaran and Morden (2007), the Aon Impact Forecasting Monte Carlo model is highlighted. They used MC methods to simulate tornado occurrence probabilities and return periods as well as potential losses for their policyholders in the United States.

### 3. TorMC model design

There are ~65 years of functional tornado data, with much of the data subject to inaccuracy and bias (e.g. Brooks *et al.*, 2003; Doswell, 2007). Even when controlling for these data issues and non-meteorological biases, small sample size remains a paramount issue for research studying the climatology of these relatively rare events (Doswell, 2007). MC simulations paired with tornado hazards (i.e. the TorMC model) do not present more accurate or realistic measures of tornado risk and climatology because their inputs remain bounded by the envelope of observed events; rather, they provide a larger ‘snapshot’ or ‘window’ of tornado event outcomes based on historical data. It is entirely plausible that, given the small sample size of observed tornado data, extremes, or ‘tails’ of the distribution, event attribute values (e.g. length, width, magnitude, count) have not been captured adequately over the last 65 years. Tornado events and their characteristics could be occurring potentially in patterns for thousands of years or more (Meyer *et al.*, 2002; Doswell, 2007). In addition, previous research examining the disaster consequences for a location have been constrained by

the number of tornado paths employed and the tornado path placement. The major advantage of the TorMC model is that it permits the estimation of regional disaster probability through tens of thousands of simulated tornado events in contrast to only a handful of outcomes. Thus, the TorMC model provides an overall better grasp of large-scale tornado risk and potential tornado impact variability.

The TorMC model comprises four general steps: (1) study region and model parameter definition; (2) tornado footprint creation; (3) tornado cost assessment, and (4) output production (Figure 1). The TorMC model was designed to be highly modular (Petersen, 2012) in order to provide a user with as many simulation options as possible. Model parameter choices are selected prior to executing the program and allow the user to control the type of output generated by the TorMC model. Model parameters, steps, considerations and caveats are discussed hereafter.

#### 3.1. Study region

The first step of the model process begins with the users defining a study domain on which they want to perform the MC simulation. The TorMC model is compatible with a study area of any shape or size (e.g. conterminous United States, state, county or custom) in shapefile (.shp) format. As illustrated by previous studies employing tornado MC methods (Meyer *et al.*, 2002; Daneshvaran and Morden, 2007), the study area size should be 80 km<sup>2</sup> or greater. This area corresponds to the Storm Prediction Center’s (SPC) probability forecasts that signify the chance of severe weather within 40 km of any point in the United States (Brooks *et al.*, 2003). Domains smaller than 80 km<sup>2</sup> may result in an underestimation of tornado occurrence within the region due to the limited observed tornado record and small sample size (~59 000 events in the conterminous United States (Doswell, 2007)).

Edge effects occur in models that sample lines with starting points, preferred azimuths and ending points that fall outside a domain (e.g. TorMC model simulated tornado paths). As the majority of tornadoes in the United States move from southwest to northeast (Suckling and Ashley, 2006), an under-sampling of tornadoes is apparent in a user-selected region’s south and west sides (Figure 2). This edge effect is removed or corrected for in the TorMC model by adding a simple 100 km buffer to the study area and thereafter sampling all events within the buffer. A clipping routine, which is discussed in a forthcoming section, is later used in the model to reclaim the user’s original domain.

#### 3.2. Tornado counts

The TorMC model attempts to simulate tornado events by using historical data acquired from the SPC SVRGIS (<http://www.spc.noaa.gov/gis/svrgis/>) data. Although there are many issues with the observed tornado data (e.g. width (Brooks, 2004; Strader *et al.*, 2015a); reporting bias (Brooks *et al.*, 2003; Doswell *et al.*, 2005; Anderson *et al.*, 2007); counts (Brooks *et al.*, 2003; Verbout *et al.*, 2006; Tippett *et al.*, 2015)), these data are the only accessible source of extensive tornado event information. The SVRGIS tornado shapefile, which contains the observed tornado record, is integrated into the TorMC model. This permits the sampling of historical event lengths, widths, years, starting locations, ending locations and magnitudes.

The number of simulated tornadoes is based on the observed SVRGIS tornado data within the user-provided study region by randomly selecting an annual tornado count from a given year in the historical data (1950–2014) using a bootstrap (Efron and

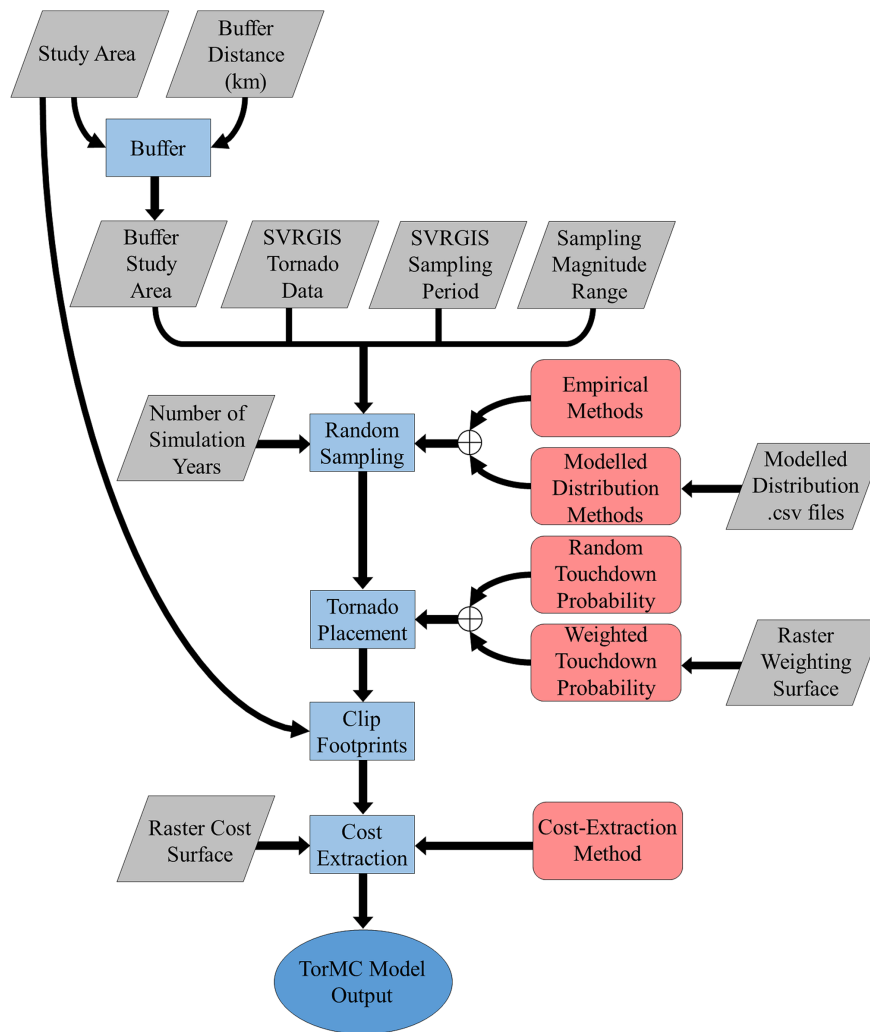


Figure 1. Tornado Impact Monte Carlo (TorMC) model flow chart. Rhombus shapes indicate model input parameters, squares represent model processes, rounded-corner rectangles denote simulation decisions or choices and the oval highlights the model output or ending process.

Tibshirani, 1994), or random sampling with replacement, technique. Although the SVRGIS data contain information as far back as 1950, annual tornado counts from 1950 to 1953 are often removed because they are considerably less complete and are of a lower quality than those from 1954 to 2014 (Agee and Childs, 2014). These abnormal counts are attributed to different sources of tornado event information (i.e. U.S. Nuclear Regulatory Commission; Grazulis, 1993) prior to the establishment of the National Severe Storms Forecast Center in 1952. Although it is preferable to remove 1950–1953 from the considered data, the user does have the capability to randomly sample randomly the annual tornado counts (adjusted or unadjusted) and their attributes from any available SVRGIS temporal range as well as other sources of data (e.g. Grazulis, 1993) that fit the SVRGIS format.

The TorMC model does not determine an exact number of tornadoes to produce; rather, it simulates years of tornado events. For instance, the model user may want to generate 10 000 years of tornado events atop a particular study region. The TorMC model would then randomly sample or select an annual tornado count from a single SVRGIS data year (1954–2014) within the study region. This randomly chosen count would then represent the total number of tornadoes the model will generate during the first year of simulation. In this case, the process would be repeated

9999 more times, with replacement, until each simulation year contains a total number of tornadoes to create. The benefit of simulating tornadoes during a given year is to capture better the inherent year-to-year variability in annual tornado occurrences across a study region.

### 3.3. Tornado magnitudes

Next, the user must also decide what magnitude of tornadoes to simulate. The user can choose to generate a single magnitude (i.e. EF0, EF1 etc.) tornado class or a range of tornado magnitudes (e.g. (EF0+), significant (EF2+) and violent (EF4+)). The TorMC model acknowledges but makes no attempt to correct for the known bias towards higher tornado intensity ratings prior to 1970 (Verbout *et al.*, 2006; Thorne and Vose, 2010; Edwards *et al.*, 2013). Future TorMC versions will accommodate and rectify any known tornado magnitude or intensity rating biases. Nevertheless, tornado occurrences are progressively rarer as magnitude increases; the TorMC model accounts for this variation by modifying the total number of tornadoes to construct in a particular simulation year. For instance, if the user wants to generate 10 000 years of violent tornadoes across the studied region, only those observed tornado events that are within the study region and meet the user-defined magnitude criteria (EF4+)

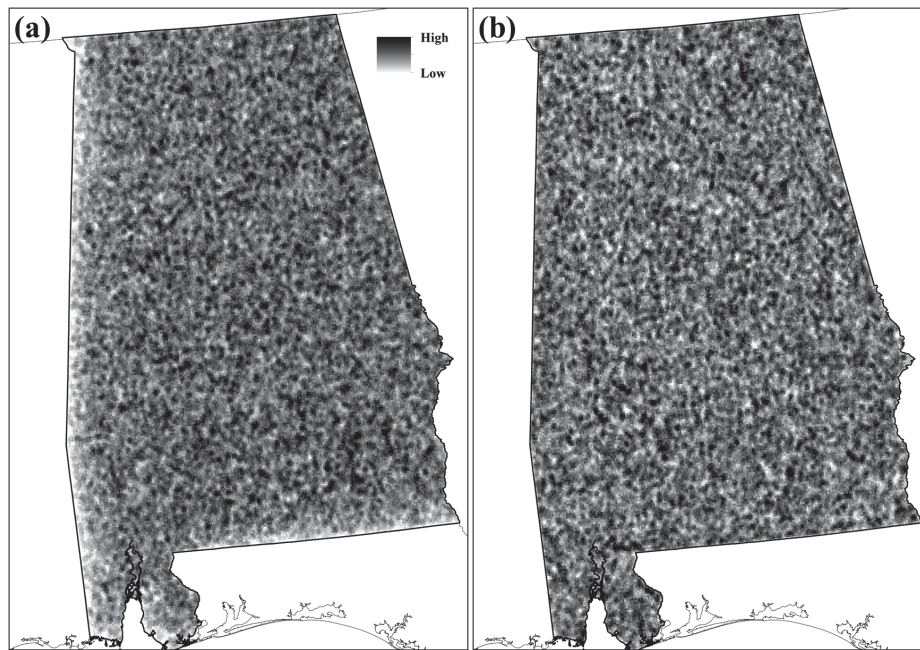


Figure 2. Point density map representing tornado ending points (longitude, latitude) from a 10 000 year Tornado Impact Monte Carlo (TorMC) simulation for the state of Alabama. (a) Illustrates the non-corrected edge effects, while (b) highlights the corrected edge effects from the buffer-clip (inflation–deflation) procedure.

will be considered in the randomly sampled SVRGIS year. This process ensures that there will not be under- or over-sampling of tornadoes at a given magnitude, while an approximate representation (based on observed record) of tornado counts by magnitude will be created for all TorMC model simulation years.

Once the TorMC model selects a random SVRGIS year and its associated observed tornado count, it then develops a second bootstrap sample to select a particular magnitude of tornado to simulate. This sampling process is then repeated until the desired total number of simulation years is reached. Bootstrap re-sampling captures the potential variability in tornado magnitudes in a year while also taking the relative percentage of all events of a given magnitude into account. For example, if a user chooses to generate significant tornado paths atop the study region from 1954 to 2014, the model will randomly select a year's significant annual tornado path count as the total number of paths to generate in the first simulation year. In this randomly chosen year, there may be 50 (30 EF2, 15 EF3, 4 EF4 and 1 EF5) significant tornadoes within the study region. The model would then randomly select one tornado magnitude, record it, place it back into the empirical data and repeat the process 49 more times until it captures a list of 50 tornado magnitudes for that simulation year. In this case, the user can expect the model to generate more EF2 than EF5 magnitude events simply based on their probability of occurrence.

#### 3.4. Tornado lengths and azimuths

Initially, the azimuths of all tornado paths within the regionally filtered SVRGIS data are calculated. An azimuth is then chosen randomly from the data based on the previously selected tornado magnitude within the study region. Because tornado azimuths are not random and have a climatological tendency to travel in particular directions in the conterminous United States (Suckling and Ashley, 2006), this process captures the character of tornado path azimuths within the study region. The procedure ensures

that a simulated tornado of a given magnitude would have its azimuth correspond to that of an observed tornado with the same magnitude in the study region. The tornado path length is also selected using this method by pairing simulated tornado lengths with observed tornado lengths within the same magnitude class. The model can also employ random sampling from model distributions (e.g. Weibull) and their fits from the observed data as opposed to sampling directly from the historical observed data.

#### 3.5. Tornado widths

Similar to Meyer *et al.* (2002) and Brooks (2004), simulated tornado path widths are determined by bootstrap sampling from a Weibull distribution fit on the observed tornado width data by tornado damage rating or magnitude in the study region. The Weibull distribution was chosen because it is non-negative and always positively skewed (Brooks, 2004). The primary advantage of using a statistical distribution (as opposed to bootstrap techniques) to model tornado path widths is that the Weibull distribution characterizes actual tornado widths better by EF scale magnitude compared with observed widths while at the same time reducing the effects of abrupt and apparent step functions in the historical tornado width data caused by systematic changes in event-recording practices. For instance, 1950–1994 tornado path widths were denoted by the mean path width and transitioned to reported maximum path widths by 1995 (Brooks, 2004; Agee and Childs, 2014; Strader *et al.*, 2015a). A second modification in tornado reporting practices occurred in 2007 with the implementation of the EF scale. Although unrelated to tornado path width reporting practices, this change to the EF scale in 2007 has produced, as a whole, wider tornado path widths. The reasons for this increase in tornado widths post EF-scale implementation are not known. To apply this modelling option, the TorMC model requires the user to provide a comma-separated values parameter file containing the alpha (shape) and beta (scale) parameters by tornado magnitude that the model calls upon to generate random

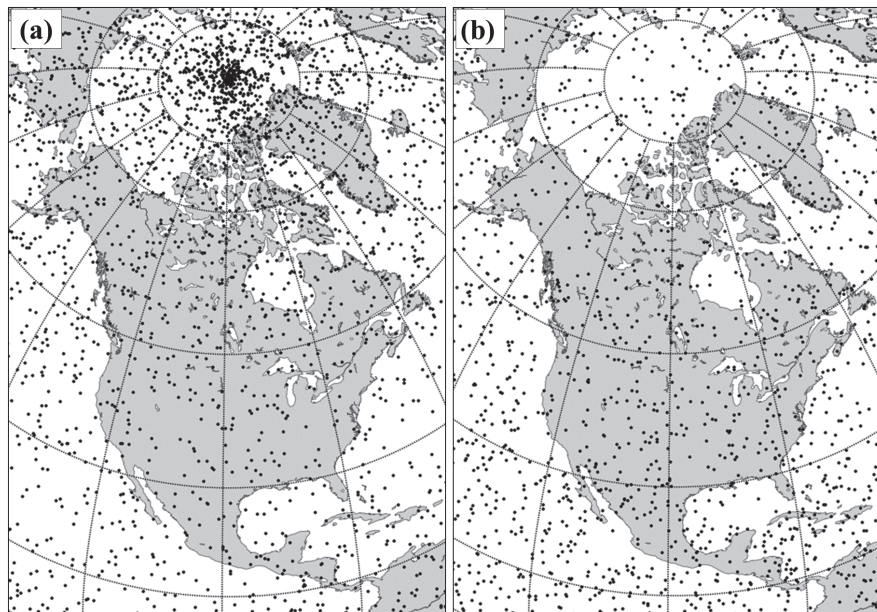


Figure 3. Shows 10 000 randomly generated longitude and latitude points on the surface of the earth. (a) Indicates the clustering of points near the poles, which results from simple uniform random generation, while (b) illustrates the spatially correct random points.

tornado widths. The model also accommodates the simulation of tornado path widths using random sampling with replacement if the user prefers this technique.

### 3.6. Tornado placement

The first tornado initiation option randomly generates latitude and longitude co-ordinates within the study region that serve as the touchdown locations for each simulated tornado. If random points are being generated on a spherical surface they will have a tendency to cluster near the poles due to converging (non-parallel) lines of longitude (Weisstein, 2002a; Figure 3). However, the TorMC model corrects for any spatial bias that may arise during this step by employing an algorithm that randomly creates latitude and longitude co-ordinates within the study area (Weisstein, 2002a). An equal tornado touchdown likelihood in the study region may be sufficient for relatively small geographical areas (e.g. regional) but potentially problematic on larger scales (e.g. conterminous United States) due to climatological differences in tornado occurrences within the United States (e.g. Dixon *et al.*, 2011; Farney and Dixon, 2014; Tippett *et al.*, 2015). Given this issue, the second tornado start location creation option considers the potential variation in tornado touchdown probability in a study region. This method requires the user to provide a tornado touchdown probability raster surface (e.g. cf. figure 4 in Brooks *et al.*, 2003) on which the start locations will be spatially weighted. The second methodology is suitable at all geographical spatial scales and provides a greater advantage in increasingly larger, user-defined study regions. The tornado event simulation portion of the TorMC model concludes with the creation of tornado footprint polygons (i.e. maximum areal extent of tornadic winds or tornado length multiplied by width) with the spatial extent and orientation controlled by the simulated path lengths, widths and azimuths.

### 3.7. Cost extraction

The cost extraction portion of the model begins with the second step in the edge correction process by clipping spatially the

tornado polygons using the original, user-defined study region. The next step employs the user-provided raster cost surface to assess the tornado impact. Prior to running the model, the user must provide the raster cost surface on which the TorMC model will calculate zonal statistics (i.e. the summarization of geospatial raster datasets based on vector geometries) using the generated tornado footprint polygons. The model accommodates any type of raster cost surface (continuous or categorical) as long as the user defines a cost field within the raster. The zonal statistics portion of the model permits a variety of statistical calculation options (e.g. mean, sum). If the user provides a raster cost surface of gridded population, a sum statistic option computes a zonal statistic representing the total number of people affected by each tornado path.

The user has the option to apply different types of cost-extraction techniques – e.g. ‘centroid within’ and ‘intersect’ (Figure 4). These methods affect the zonal statistics calculation for each tornado footprint. The centroid within extraction method calculates zonal statistics solely for those raster cells where the tornado footprint intersects the centroid of the cell, while the intersect extraction technique includes all the raster cells that are touched by a tornado footprint in the zonal statistics calculation. Although not a part of this TorMC iteration, the ‘completely within’ and ‘areal weight’ techniques provide additional means of cost extraction. The completely within method includes all raster cells that are contained within the bounds of the tornado footprint. The areal weight (AW) method (Schlossberg, 2003; Balk *et al.*, 2005; SEDAC, 2015; Ashley *et al.*, 2014) provides a more accurate measure of tornado costs, especially for those grid cells along the edges of the tornado footprint. Where a tornado footprint transects portions of grid cells, cost tallies (e.g. HUs) are adjusted based on the areal fraction of the grid cells affected (Figure 4). For example, if a tornado path bisects a grid cell representing 100 HUs, then the total number of HUs impacted by the tornado in that grid cell is 50 (i.e.  $0.50 \times 100 \text{ HU} = 50 \text{ HUs}$ ). This process is then repeated for all grid cells that the tornado footprint traverses. Each cost-extraction technique is heavily influenced by the spatial

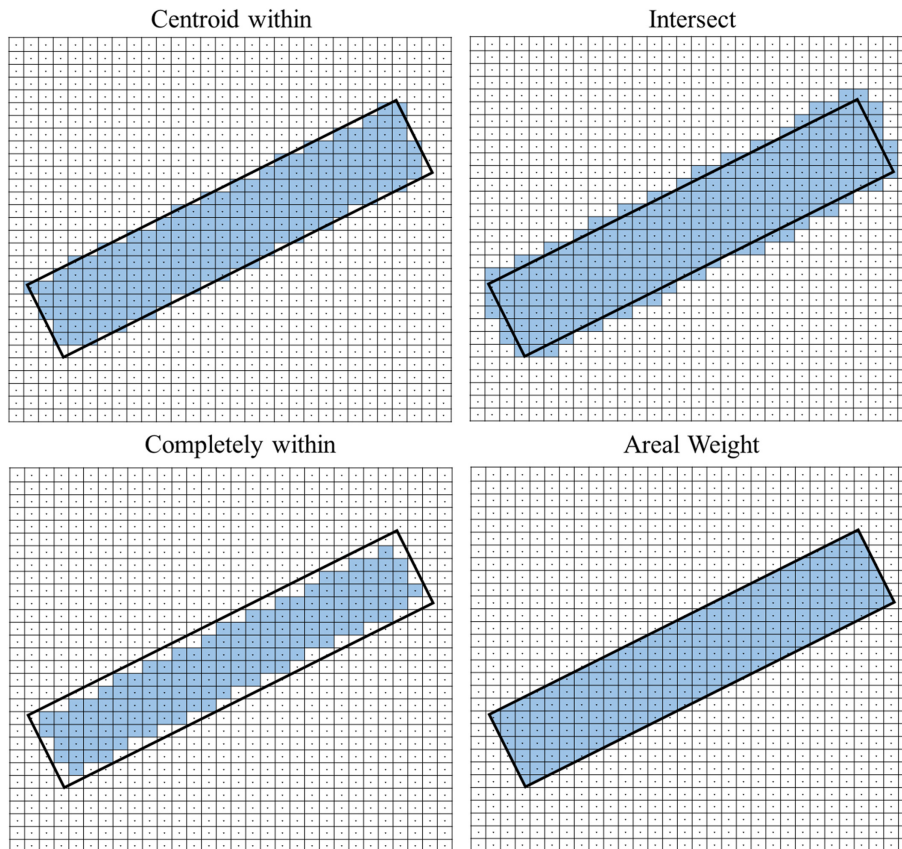


Figure 4. Illustration of centroid within, intersect, completely within and areal weighted (AW) cost-extraction techniques. The grid cells represent the cost surface with black dots comprising the centroid of each cell, and the non-shaded rectangle signifies a potential tornado footprint. Shaded grid cells indicate those that would be included in the tornado cost calculation during each type of cost-extraction method (after Schlossberg, 2003).

resolution, or cell size, of the raster cost surface. For instance, a raster surface with low spatial resolution in combination with the centroid method would result in an underestimation of tornado costs. In general, a raster with a high spatial resolution will lead to superior estimates of impact.

### 3.8. Model output

The TorMC model yields both .shp and .csv files representing the TorMC geo-dataframe with various simulation data fields. Fields generated include unique tornado field identifier (FID), projected footprint polygon geometry, starting latitude and longitude, ending latitude and longitude, path length (km) and width (km), azimuth ( $^{\circ}$ ), magnitude (0–5), simulation year and zonal statistics.

## 4. TorMC model application

### 4.1. Model performance

To illustrate the model's reliability and performance, a simulation based on 10 000 years of significant tornadoes across the state of Oklahoma was conducted initially. Significant tornadoes were simulated as they have been responsible for 98.8% of all tornado fatalities and a majority of tornado damage since 1950 (Ashley, 2007; Simmons and Sutter, 2007). In addition, significant tornado event frequency has remained consistent since 1950, while non-significant tornado event frequency has risen substantially due to non-meteorological influences (e.g. Doswell, 2007).

Oklahoma is a suitable candidate for examining model performance due to its elevated significant tornado risk and relatively large population centres exposed to this risk (e.g. Oklahoma City and Tulsa). After testing a variety of simulation lengths, 10 000 years was a period of record that produced functional, yet computationally efficient, output. The 10 000 year significant tornado simulation was coupled with a gridded, fine-scale (100 m) residential built-environment cost surface, representing HUs across Oklahoma in the year 2010. The HU cost surface is derived from the Spatially Explicit Regional Growth Model (SERGoM; Theobald, 2005), which employs a variety of geospatial data such as water bodies, protected areas, Census block population, road density, etc., to determine HU density at the 100 m scale in the conterminous United States. SERGoM data accuracy and reliability were measured using a hindcast technique, with the model output comparable to Census data (Theobald, 2005).

Tornado counts from 1954 to 2014 were considered, while tornado widths were modelled using the Weibull parameters outlined by Brooks (2004). Tornado lengths, azimuths and magnitudes were selected using a bootstrap sampling technique on the observed tornado data. For the present study, a random tornado touchdown probability coupled with the intersect cost-extraction method was used although it may remove any potential climatological patterns of tornado occurrence and attributes. However, a potential benefit in using this tornado placement technique is that it avoids tornado reporting bias that may be, in part, due to population density (e.g. Doswell *et al.*, 2005). This bias is evident when comparing observed significant tornadoes (Figure 5(a)) to the randomly chosen 61 simulation years (Figure 5(b)). In

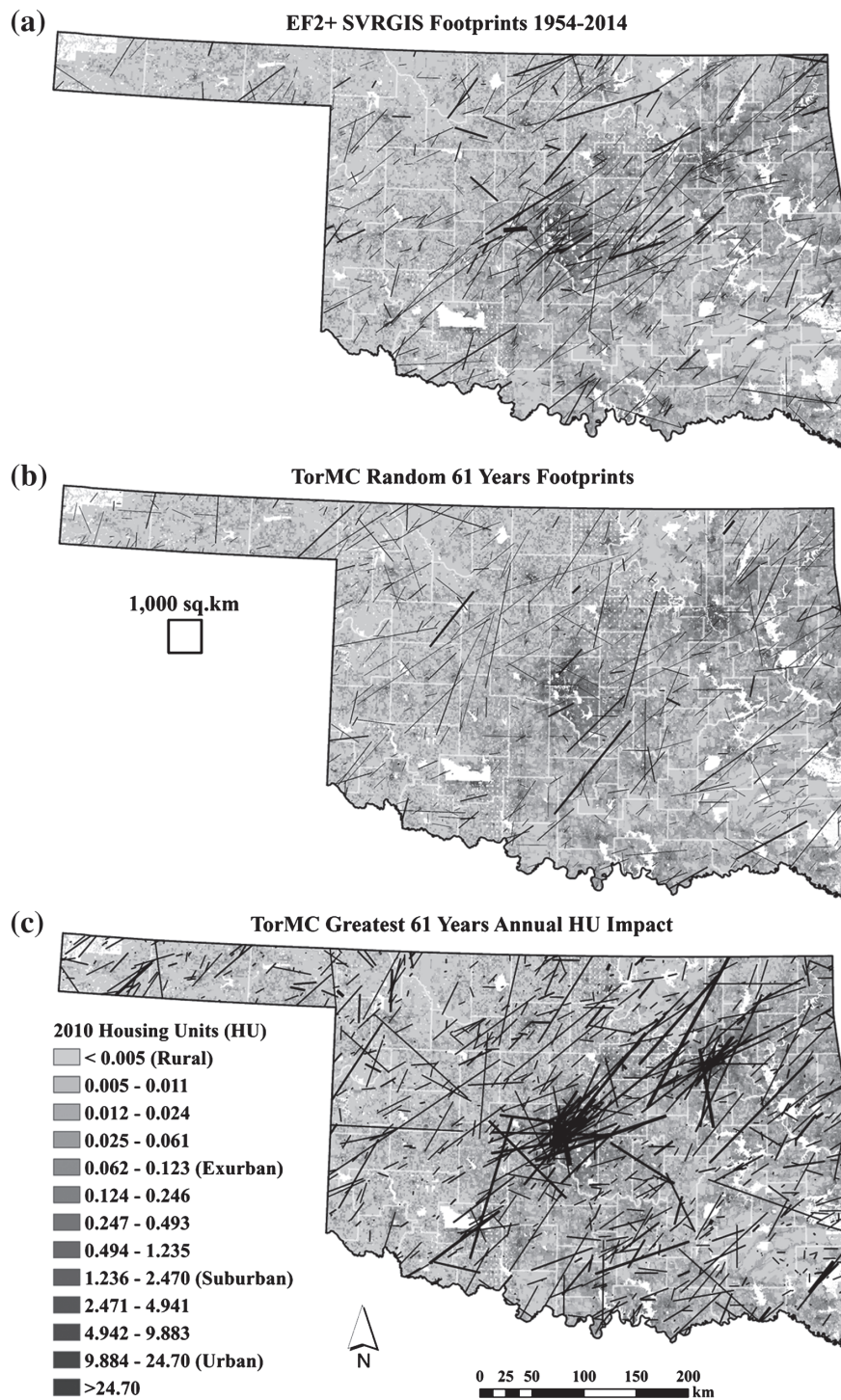


Figure 5. (a) Observed SVRGIS significant (EF2+) tornado footprints from 1954 to 2014 (dark black lines) with the SERGoM total number of housing units (HU) *per* ha in 2010 for the state of Oklahoma. (b) Same as in panel (a) but with a random 61 years of simulated significant tornado footprints. (c) Same as in panel (a) except for the TorMC's 10 highest annual HU impact years. The period of 61 years was selected because that was the temporal range of observed historical events used in the Tornado Impact Monte Carlo (TorMC) simulations.

this case, clustering of significant tornado footprints around the Oklahoma City metropolitan area is apparent in the observed historical tornado data, while the TorMC-simulated footprint placement illustrates a random pattern.

Over the 10 000 year simulation, the TorMC model generated 116 045 significant tornadoes, with 73.8% EF2, 20.6% EF3, 5.1% EF4 and 0.6% EF5 tornadoes (Table 1). The simulated percentages of tornadoes by EF magnitude are similar to those from

Oklahoma's observed record from 1954 to 2014 (i.e. 71.6% EF2, 21.2% EF3, 6.3% EF4 and 0.9% EF5). The model produced a mean (median) of 11.6 (10) significant tornadoes *per* year over the 10 000 year simulation with a violent tornado occurring every 1.5 years (Table 2). This represents a 66% chance a violent tornado will traverse Oklahoma in a given simulation year. A random sample of 61 years was chosen from the 10 000 year simulation (sample period) and compared to the observed tornado

Table 1. Significant and violent tornado attributes from the 10 000 year TorMC model simulation for the state of Oklahoma. Tornado EF magnitude, count, mean annual count, mean length, mean width, mean azimuth are denoted.

Magnitude	Count	Mean annual count	Mean length (km)	Mean width (m)	Mean azimuth (°)
EF2	85 645	8.56	12.01	122.44	66.89
EF3	23 846	2.38	25.64	262.45	66.08
EF4	5919	0.59	51.19	457.40	67.21
EF5	635	0.06	63.87	551.45	67.58
EF2+ (Significant)	116 045	11.60	17.09	170.64	66.74
EF4+ (Violent)	6554	0.66	52.42	466.51	67.25

Table 2. TorMC model results from a 10 000 year simulation of significant tornadoes atop the state of Oklahoma. Tornado event EF magnitude, return period, annual occurrence probability, the mean number of HUs affected by a given tornado and the mean number of HUs impacted by all tornadoes in a simulation year are indicated.

Magnitude <sup>a</sup>	Return period (years)	Annual occurrence probability	Mean tornado impact (HU)	Mean annual impact (HU)
EF2	0.12	8.56	24.53	210.07
EF3	0.42	2.38	73.62	175.56
EF4	1.69	0.59	205.84	121.84
EF5	15.75	0.06	306.76	19.48
EF2+ (Significant)	0.09	11.60	45.41	526.94
EF4+ (Violent)	1.53	0.66	215.62	141.32

<sup>a</sup>Given the distribution of tornadic winds within a footprint, only a small percentage of the total HUs affected by the tornado footprints are subject to significant or violent tornado wind speeds (e.g. Strader *et al.*, 2015a).

data of 1954–2014 (observed period). Comparisons between the sample and observed record revealed a consistent median number of significant tornadoes *per year* (11), while the mean number of significant events *per year* was 14.6 and 12.1 for the observed and sample periods, respectively. The statistical difference between the randomly sampled 61 simulated years and observed years is attributed to the year-to-year variability of simulated significant tornado counts. The percentages of tornadoes by EF magnitude for the observed (71.6% EF2; 21.2% EF3; 6.3% EF4; 0.9% EF5) and sampled (73.2% EF2; 21.0% EF3; 4.3% EF4; 1.5% EF5) periods are also similar, revealing that the TorMC model data mirrors the observed data.

The 10 000 year Oklahoma simulation generated mean significant tornado length and width of 17.1 km and 170.6 m, respectively (Table 1). Compared to the observed data, and as illustrated in Brooks (2004) and Strader *et al.* (2015a), tornado length and width typically increase as EF magnitude escalates. Mean tornado lengths for significant tornadoes ranged from 12 km (EF2) to 63.9 km (EF5), while mean tornado widths varied from 122.4 m (EF2) to 551.5 m (EF5). All mean simulated tornado lengths by EF magnitude are within 5 km of the corresponding empirically sampled data. Mean simulated tornado path widths by EF magnitude are all within 5 m of the Brooks (2004) mean modelled tornado widths by EF magnitude (cf. figure 2 in Brooks, 2004). Simulated tornado azimuths closely resemble those of the sample observed tornado data with the mean simulated path azimuth for all significant tornado paths at 66.7° (slightly west of southwest to east-northeast), which aligns with the observed azimuths found in the south central U.S. region (cf. figure 5 in Suckling and Ashley, 2006).

Using the 2010 SERGoM cost surface, the mean (median) number of HUs affected by a single significant tornado footprint is 45.4 (2.2) (Table 2). Mean HU impacts are much larger than median impacts because of the rare and ‘extreme’ distribution nature of the TorMC model POE curves (Figure 6). As a majority of tornadoes do not traverse developed landscapes (e.g. people and HUs), mean HU impacts are influenced much more by high-end (POE < 0.1) simulation years compared with the

median. Because of this, the median HU impacts are a more desirable central tendency metric.

Similar to the TorMC model length and width results, as the EF scale magnitude increases, the mean number of HUs impacted by a tornado footprint is amplified. Violent tornado footprints affected a mean (median) of 215.6 (25.1) HUs *per* tornado footprint. Because violent tornadoes are, on average, longer-tracked and wider, they often affect an exponentially greater number of HUs compared with non-violent tornadoes. In fact, ranking the tornado footprints by the number of HUs they affected reveals that 20 out of the top 25 individual tornado impact values originated from violent events. However, aggregating or grouping the individual tornado footprint costs to an annual sum indicates that significant tornadoes affect a greater number of HUs on average (mean and median) over a given simulation year compared with violent tornadoes (Table 2). This is attributed to the more frequent occurrence of EF2 and EF3 tornadoes compared with EF4 and EF5 tornadoes. While tornado length and width play an important role in individual tornado impacts, the annual number of HUs affected is influenced more heavily by significant tornado frequency. For instance, TorMC-modelled significant events affected a mean of 526.9 HUs *per* simulation year, whereas violent footprints affected a mean of 141.32 HUs *per* simulation year. It should be noted that although this TorMC simulation example employs significant tornadoes as a measure of tornado exposure, regions of greater rural land concentration (Oklahoma) can lead to an underestimation in tornado intensity (e.g. Doswell *et al.*, 2009) and/or counts (e.g. Brooks *et al.*, 2003). This is attributed primarily to the lack of people to witness and report a tornado event as well as an absence of damage indicators necessary for estimating tornadic winds in rural areas (Doswell *et al.*, 2009).

Statistical measures, such as POE curves, are often used to gauge the likelihood of hazard occurrence by intensity or magnitude. A POE curve of the annual HU impacts for the state of Oklahoma in 2010 reveals that the mean (median) annual number of HUs impacted by significant tornadoes is 526.9 (183.7) (Figure 6). The difference between the mean and median values

suggests that the mean is influenced heavily by the simulation years where significant tornadoes affected a large number of HUs. The maximum annual number of HUs impacted for the 10 000 year simulation was 35 922. During this hypothetical year, a 2.6 km wide, 38.6 km long EF4 tornado traversed the Oklahoma City metropolitan area, affecting over 34 884 HUs. This particular simulated tornado contained a total footprint area of 100.36 km<sup>2</sup>, which is over four times the impact size of the 2013 Newcastle-Moore EF5 tornado footprint (23.6 km<sup>2</sup>). It also impacted nine times as many HUs as the 2013 Newcastle-Moore tornado (3829 HUs). As expected, simulation years where a significant or violent tornado footprint traversed highly populated areas resulted in a large number of annual HUs affected (Figure 5(c)). The standard deviation of the annual number of HUs impacted for all 10 000 simulation years is 1130.2, and the co-efficient of variation is 214.5%, suggesting that the yearly impact sums are also highly variable.

#### 4.2. Comparison of Alabama, Illinois and Oklahoma POE Measures

To demonstrate model cost-extraction performance further, POE curves for two additional states (Alabama and Illinois) were created using the same TorMC model parameters as the Oklahoma simulation (Figure 6). These states were chosen because of their relatively high tornado risk and differing exposure character. This provides the opportunity to examine how changes in risk and exposure manifest in tornado disaster potential for different geographical regions. Oklahoma is situated in the heart of what is colloquially known as Tornado Alley (cf. Brooks *et al.*, 2003; Dixon *et al.*, 2011), where significant tornado occurrence risk is high (Smith *et al.*, 2012; Tippett *et al.*, 2015), and population density is clustered mostly within a few metropolitan areas. Alabama has a high significant tornado risk (Coleman and Dixon, 2014) with elevated tornado exposure due to a relatively high population density compared with Oklahoma. Illinois features a mixture of the disaster constituents found in the other state samples, with a large population density and moderate-to-high significant tornado risk. The three POE curves represent the TorMC-simulated annual number of HUs impacted by significant tornado footprints *per* 1000 km<sup>2</sup> using a 2010 SERGoM HU cost surface (Figure 6). The POE curves are normalized by their individual state areas (km<sup>2</sup>) to control for differences in state size.

The POE curves highlight the effects of tornado exposure (HU density and distribution) and risk (significant tornado frequency, length, width, magnitude, etc.) on annual impact probabilities. Oklahoma contained the greatest number of simulated significant events due to its higher significant tornado occurrence compared with Illinois and Alabama (Table 3; Figure 7). Additional annual HU impact statistics such as the median, 25<sup>th</sup> percentile, 75<sup>th</sup> percentile, mean, standard deviation and maximum annual number of HUs affected by significant tornadoes capture underlying differences in state tornado risk and vulnerability as well as the relative contributions of each constituent to disaster potential. Comparing the three states, Oklahoma contains the largest number of simulated tornadoes, while Alabama encompasses the highest mean annual simulated EF2+ footprint area. However, upon examining each state's mean annual number of HUs impacted *per* 1000 km<sup>2</sup>, Illinois has the greatest (10.4) mean annual HU impact, followed by Alabama (7.16) and Oklahoma (2.93). This result suggests that although some of the dissimilarities in annual HUs affected in each state can be attributed to different tornado frequency and footprint risks (i.e. EF2+ tornadoes have affected 108.3 km<sup>2</sup> *per* year on average (mean) in

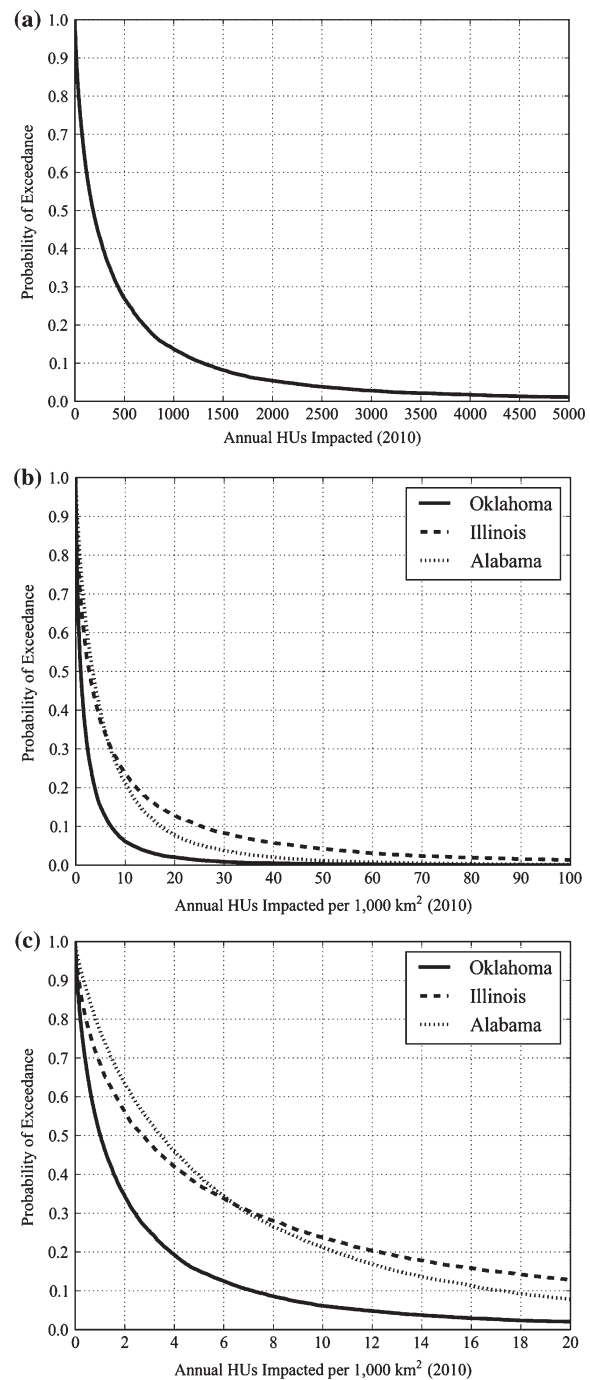


Figure 6. (a) Probability of exceedance (POE) curve comprising a 10 000 year simulation of the annual number of housing units (HUs) affected by significant tornadoes throughout the state of Oklahoma. (b) Same as in panel (a) but Oklahoma (solid line), Illinois (dashed line) and Alabama (dot line) POE curves represent the annual number of affected HUs normalized by state area (1000 km<sup>2</sup>). (c) Same as in panel (b) but zoomed in to highlight 20 or less annual number of HUs impacted by tornadoes.

Alabama from 1954 to 2014 compared with Oklahoma (101.3 km<sup>2</sup>) and Illinois (42.5 km<sup>2</sup>)), a majority of the disparity in the tornado annual impacts in Alabama, Illinois and Oklahoma can be attributed largely to the overall number of 2010 HUs that are exposed to simulated significant tornado events in each state. For instance, Illinois contains more HUs (4 132 154) than Oklahoma (1 903 946) and Alabama (2 293 091) because of the very large

Table 3. The annual number of affected housing units (HUs) normalized by state (Alabama, Illinois and Oklahoma) area (1000 km<sup>2</sup>) for 10 000 TorMC model simulations using the 2010 SERGoM HU cost surface.

State	Normalized EF2+ count	25 <sup>th</sup> Percentile	Median	75 <sup>th</sup> Percentile	Mean	Standard deviation	Maximum
Alabama	643	1.14	3.48	8.57	7.16	12.40	445.53
Illinois	600	0.64	2.73	9.33	10.40	25.89	590.97
Oklahoma	641	0.29	1.02	3.04	2.93	6.26	198.42

The number of simulated significant tornadoes normalized by state area (tornadoes *per* 1000 km<sup>2</sup>) as well as the 25<sup>th</sup> percentile, median, 75<sup>th</sup> percentile, mean, standard deviation and maximum annual number of HUs affected *per* 1000 km<sup>2</sup> are represented.

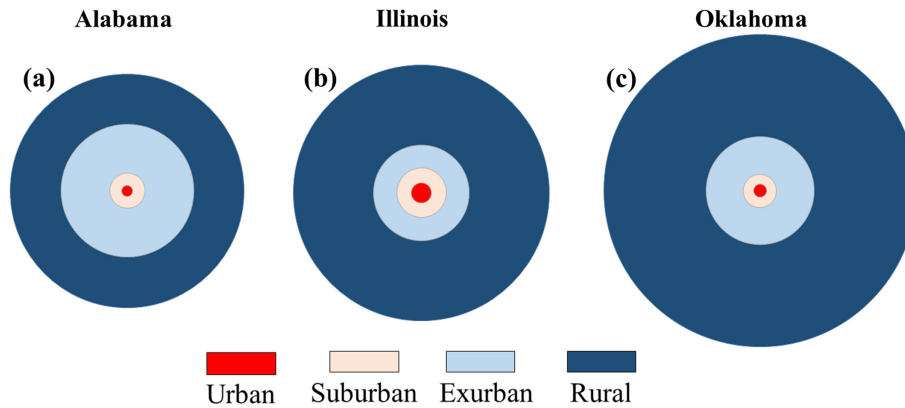


Figure 7. Panels (a)–(c) illustrate the percentage of total state developable area by land use (LU) classification (rural (>16.18 hectares (ha) *per* HU); exurban (0.8–16.18 ha *per* HU); suburban (0.1–0.8 ha *per* HU); and urban (<0.1 ha *per* HU); Theobald, 2005; cf. Table 4). The size of each circle is scaled by the total developed land area in each individual state.

and densely populated Chicago metropolitan area in addition to a number of other smaller metropolitan regions. Breaking down the total number of HUs by land use (LU) classification reveals that Illinois contains ~2.2 million HUs more than Oklahoma and Alabama in the urban and suburban LU classification (Table 4). The annual HU impact POE curves are largely influenced by whether a state contains a highly populated metropolitan area with a large number of HUs. As illustrated by the Illinois curve (Figure 6), a region encompassing a location with a large number of HUs has a tendency to ‘pull’ the POE curve tail towards greater magnitude impact values. This results in more variability (i.e. higher standard deviation) in the annual significant tornado impact values. Those regions with relatively fewer HUs cause the POE curve to ‘decay’ much more quickly, effectively shifting the tail of the POE curve towards lower magnitude impact values.

The differences in the mean annual HU impacts of Alabama, Illinois and Oklahoma can be explained largely by the variation in the total number of HUs in each state and whether the state contains a highly populated metropolitan area dominated by urban and suburban LU. However, the 25<sup>th</sup> and 50<sup>th</sup> (median) percentiles of the POE curves indicate how rural and exurban LU influence the tornado disaster potential (Tables 3 and 4; Figure 6). Although Illinois has the greatest mean annual HU impacts compared with the other two states, Alabama has the highest (3.48) median annual HU impacts. As exemplified in Figure 6(c), the POE curve associated with Alabama outpaces the Oklahoma and Illinois curves until approximately 6.5 annual HUs are impacted *per* 1000 km<sup>2</sup> when the Illinois curve surpasses the Alabama curve. This effect can be attributed to the difference in the Illinois and Alabama rural and exurban LU or, more generally, how the HUs are distributed across all LU classes (Table 4). A large majority (91.6%) of Illinois HUs are under the urban and suburban LU classification, while only 8.4% are situated in rural or exurban development. However, 31.5% of the

total HUs in Alabama is classified as rural or exurban development type, suggesting that the spatial pattern of Alabama’s residential built-environment is much more dispersed than that of Illinois (Figure 6). Evidence of this pattern is also illustrated when investigating the percentage of total developed area in relation to the percentage of total HUs by LU classification. Alabama, Illinois and Oklahoma all contain approximately the same percentages (96–99%) of rural and exurban LU area, but Alabama has approximately 30% of its total 97% rural–exurban development in the exurban classification compared with Illinois (10.2%) and Oklahoma (10.7%). The net effect of this difference manifests in the total number of HUs in the exurban LU classification for each state; Alabama has 32 000 and 41 000 more HUs in exurban LU than Illinois and Oklahoma, respectively.

Overall, the comparison of the Alabama, Illinois and Oklahoma POE curves show how tornado risk plays a minor role in annual HU impacts, while disaster severity and frequency is more often controlled by exposure, or physical vulnerability, attributes. More specifically, the magnitude of total population and HUs, as well as how it is distributed in geographical space, determine the tornado hazard consequences and the disaster magnitude.

#### 4.3. Incorporating and measuring spatiotemporal changes in tornado risk and exposure

Subsequent iterations and applications of the TorMC model will encourage stakeholders to assess how tornado disaster potential has changed or may evolve in the future given the continual development and potential changes in environments supportive of tornadoes. By supplying the TorMC model with a risk surface weighted by future potential shifts in severe weather environments (e.g. Trapp *et al.*, 2007; Diffenbaugh *et al.*, 2013; Gensini and Mote, 2014, 2015) and/or those researchers examining future

Table 4. Developed land use classification for the 2010 SERGoM raster cost surface by state (Alabama, Illinois and Oklahoma).

State	LU	Total HU	Percentage of total HU	Total developed area (km <sup>2</sup> )	Percentage of total developed area
Alabama	Rural	64 197	2.80	84 383	67.57
	Exurban	657 708	28.68	37 763	30.24
	Suburban	655 165	28.57	2447	1.96
	Urban	916 020	39.95	289	0.23
	Total	2 293 091	100.00	124 882	100.00
Illinois	Rural	98 969	2.40	117 642	86.09
	Exurban	246 661	5.97	13 931	10.19
	Suburban	710 965	17.20	4216	3.08
	Urban	3 075 558	74.43	873	0.64
	Total	4 132 154	100.00	136 661	100.00
Oklahoma	Rural	92 420	4.85	147 321	88.11
	Exurban	332 987	17.49	17 991	10.76
	Suburban	607 657	31.92	1596	0.95
	Urban	870 882	45.73	295	0.18
	Total	1 903 946	100.00	167 203	100.00

Total housing units (HUs), percentage of total HUs, total developed area (km<sup>2</sup>), percentage of total developed area by land use (LU)-developed classification. LU classes are defined as rural (>16.18 hectares (ha) *per* HU); exurban (0.8–16.18 ha *per* HU); suburban (0.1–0.8 ha *per* HU); and urban (<0.1 ha *per* HU) (Theobald, 2005).

population growth, development or LU change (e.g. Bierwagen *et al.*, 2010), a more complete grasp of future tornado disaster potential in a warming, and rapidly developing, world may be reached. The spatiotemporal comparison of POE curves generated from historical risk and/or exposure surfaces and potential future risk and/or exposure surfaces allows for the estimation of changes in future tornado impact potential, frequency and magnitude. This type of analysis is in line with the directives from the Intergovernmental Panel on Climate Change (IPCC) Special Report on Managing the Risks of Extreme Events and Disasters to Advance Climate Change Adaptation (SREX), which calls for research to improve the understanding of future climate risk and extremes. The development of tools (i.e. non-stationary extreme value analysis methods), especially those on a small scale, supports efforts aimed at increasing knowledge about future climate events (Wilby, 2007).

## 5. Conclusion and discussion of future improvements

As the tornado disaster landscape continues to change due to population growth and residential and commercial development and possible shifts in environments supportive of hazardous convective weather (Tippett *et al.*, 2015), new tools for investigating the potential consequences associated with the hazard are needed (van de Walle and Turoff, 2007; Pelletier *et al.*, 2015). The Tornado Impact Monte Carlo (TorMC) model presented permits the assessment of tornado disaster likelihood and severity in a region. Illustrations of the model reveal the tool's capacity for exploring and understanding how tornado risk and vulnerability intermingle at a location to estimate the disaster potential. This capability may assist emergency managers, planners, insurers and decision makers in their development of disaster mitigation, response and recovery strategies for their communities.

Meyer *et al.* (2002) and Daneshvaran and Morden (2007) paved the way for research that employed Monte Carlo (MC) approaches in examining the tornado hazard and associated impacts on society. The TorMC model incorporates elements from both Meyer *et al.* (2002) and Daneshvaran and Morden (2007) to estimate tornado impacts and disaster potential for a region. Continued development of the TorMC model will improve its efficiency by incorporating new and refined methods

and expand its utility. As outlined by Meyer *et al.* (2002), one cannot assume that real, small-scale tornado features are constant throughout the United States. Although the TorMC model captures regional variability in tornado risk attributes (e.g. frequency, magnitude, length, width, azimuth), this process could be improved potentially as the observed tornado record lengthens and new model techniques are implemented.

The iteration of the TorMC model only simulates theoretical tornado footprints that represent potential worst-case tornado spatial dimensions (i.e. generated length multiplied by width). Obviously, this is not the most accurate depiction of actual tornado coverage as tornado intensity, width and azimuth vary greatly as it traverses a landscape (Strader *et al.*, 2015a). Daneshvaran and Morden (2007) use a formula acquired from Twisdale *et al.* (1981) to determine how tornado wind speed and the inferred damage intensity fluctuate throughout its life cycle. Similarly, future TorMC model iterations will integrate tornado intensity distributions (TID) (Strader *et al.*, 2015a) in conjunction with a weighted 'random walk' method (Weisstein, 2002b) to capture better how tornado intensity, width and azimuth change as the tornado navigates a setting.

Future TorMC versions will be able to ingest vector cost surfaces, which will permit the implementation of the areal weighting tornado cost-extraction method. This type of modularity will enable the model to simulate events atop any type of spatial surface while also improving tornado impact estimates at any spatial and temporal resolution. As vector data are a primary source of geospatial information, the integration of this data structure will enhance the overall applicability and versatility of the model.

The Storm Prediction Center (SPC) has issued probabilistic severe weather forecasts since 2000 and has given a number of directives aimed at estimating potential severe weather impacts on society (e.g. Smith *et al.*, 2015a). Recent forecasting methods tested at the National Oceanic and Atmospheric Administration Hazardous Weather Testbed have illustrated the effectiveness of probabilistic forecasting techniques for severe convective weather (Karstens *et al.*, 2015; Smith *et al.*, 2015b). Many of the TorMC model methods and techniques could be integrated into ongoing research-to-operations initiatives at the SPC to improve probabilistic societal impact estimation and resolution of the model, and user confidence. In order to make this possible,

improving the functionality and accuracy of the TorMC model for shorter than annual time periods (i.e. seasonal, monthly, weekly and daily) is needed. Such processes will require both subjective user (e.g. forecaster) input and testing as well as the continued advancement in research, employing numerical forecast guidance (e.g. proxy severe weather reports using the National Center for Environmental Prediction's (NCEP) High-Resolution Rapid Refresh (HRRR) model; Trapp *et al.*, 2011; Gensini and Mote, 2014) to approximate fine-scale, local, severe weather occurrences.

The TorMC model has a number of potential applications beyond this initial investigation. The methods and techniques used in the development of this model could be expanded to a variety of other geophysical hazards such as severe non-tornadic wind, hail, tropical cyclones, flooding, volcanic eruptions, earthquakes, to improve the overall understanding of how these hazards interact with and impact society. Because of this applicability, future work regarding the TorMC model choices and implications will be illustrated through a user guide or manual. This manual will enable users to apply the TorMC model in their own research efficiently.

Models employing similar computational strategies to the TorMC may spur disaster mitigation and response strategies on the local, state and national scales. The adaption, improvement and enforcement of land-planning policies could increase the resilience while reducing the hazard risk (e.g. Mann *et al.*, 2014; IPCC, 2014). For example, the implementation of tornado safe rooms or tornado shelters and adaption of building codes may enhance tornado survivability and decrease disaster consequences in tornado-prone areas (Simmons and Sutter, 2007; Prevatt *et al.*, 2012; Simmons *et al.*, 2015). Restricting new development near uncertain and dynamic floodplains (Patterson and Doyle, 2009), seismically and volcanically active areas (Strader *et al.*, 2015b), locations prone to wildfires (Bryant and Westerling, 2014; Mann *et al.*, 2014), regions subject to tropical cyclone hazards and sea-level rise (Pielke *et al.*, 2008; Maloney and Preston, 2014) may reduce disaster losses. As decision makers, emergency managers and land use (LU) planners actively incorporate disaster potential into their policies and strategies and invest in those strategies, hazard impacts could be decreased and potential disasters averted.

## Acknowledgements

The authors would like to thank the anonymous reviewers whose suggestions improved the manuscript significantly. They also thank Dr. Andrew Krmencic and Mr. Alex Haberlie for their comments and suggestions on earlier versions of this model and manuscript. Lastly, the authors wish to thank Dr. David Changnon and the Meteorology Program/Geography Department Research Fund for supporting this research.

## References

- Agee E, Childs S. 2014. Adjustments in tornado counts, F-scale intensity, and path width for assessing significant tornado destruction. *J. Appl. Meteorol. Climatol.* **53**(6): 1494–1505.
- Anderson C, Wickle C, Zhou Q, Royle J. 2007. Population influences on tornado reports in the United States. *Weather Forecast.* **22**(3): 571–579.
- Apel H, Thielen A, Merz B, Blöschl G. 2004. Flood risk assessment and associated uncertainty. *Nat. Hazards Earth Syst. Sci.* **4**(2): 295–308.
- Ashley W. 2007. Spatial and temporal analysis of tornado fatalities in the United States: 1880–2005. *Weather Forecast.* **22**: 1214–1228.
- Ashley W, Strader S. 2015. Recipe for disaster: how the dynamic ingredients of risk and exposure are changing the tornado disaster landscape. *Bull. Am. Meteorol. Soc.* DOI: 10.1175/BAMS-D-15-00150.1.
- Ashley W, Strader S, Rosencrans T, Krmencic A. 2014. Spatiotemporal changes in tornado hazard exposure: the case of the expanding bull's eye effect in Chicago, IL. *Weather Clim. Soc.* **6**: 175–193.
- Balk D, Brickman M, Anderson B, Pozzi F, Yetman G. 2005. Mapping global urban and rural population distributions: Estimates of future global population distribution to 2015. Center for International Earth Science Information Network, Socioeconomic Data and Applications Center, Columbia University, 77 pp. [http://sedac.ciesin.columbia.edu/gpw/docs/GISn.24\\_web\\_gpwAnnex.pdf](http://sedac.ciesin.columbia.edu/gpw/docs/GISn.24_web_gpwAnnex.pdf) (accessed 5 May 2015).
- Bierwagen B, Theobald D, Pyke C, Choate A, Groth P, Thomas J, et al. 2010. National housing and impervious surface scenarios for integrated climate impact assessments. *Proc. Natl. Acad. Sci. U. S. A.* **107**(49): 20887–20892.
- Bouwer L. 2011. Have disaster losses increased due to anthropogenic climate change? *Bull. Am. Meteorol. Soc.* **92**: 39–46.
- Brooks H. 2004. On the relationship of tornado path length and width to intensity. *Weather Forecast.* **19**: 310–319.
- Brooks H, Doswell C III, Kay M. 2003. Climatological estimates of local daily tornado probability. *Weather Forecast.* **18**: 626–640.
- Bryant B, Westerling A. 2014. Scenarios for future wildfire risk in California: links between changing demography, land use, climate, and wildfire. *Environmetrics* **25**: 454–471.
- Burkett V, Davidson M. 2012. Coastal impacts, adaptation and vulnerability: a technical input to the 2012 National Climate Assessment. Cooperative Report to the 2013 National Climate Assessment, Island Press Washington, DC: 150 pp.
- Changnon S, Pielke R Jr, Changnon D, Sylves R, Pulwarty R. 2000. Human factors explain the increased losses from weather and climate extremes. *Bull. Am. Meteorol. Soc.* **81**: 437–442.
- Coleman T, Dixon P. 2014. An objective analysis of tornado risk in the United States. *Weather Forecast.* **29**(2): 366–376.
- Cutter SL, Emrich CT, Webb JJ, Morath D. 2009. Social vulnerability to climate variability hazards: a review of the literature. Final Report to Oxfam America. University of South Carolina, Columbia, SC: 44 pp.
- Daneshvaran S, Morden R. 2007. Tornado risk analysis in the United States. *J. Risk Finance* **8**(2): 97–111.
- Diffenbaugh N, Scherer M, Trapp R. 2013. Robust increases in severe thunderstorm environments in response to greenhouse forcing. *Proc. Natl. Acad. Sci. U. S. A.* **110**: 16361–16366.
- Dixon P, Mercer A, Choi J, Allen J. 2011. Tornado risk analysis: is Dixie Alley an extension of tornado alley? *Bull. Am. Meteorol. Soc.* **92**: 433–441.
- Doswell C III. 2007. Small sample size and data quality issues illustrated using tornado occurrence data. *Electron. J. Severe Storms Meteorol.* **2**(5): 1–16.
- Doswell C III, Brooks H, Kay M. 2005. Climatological estimates of daily local nontornadic severe thunderstorm probability for the United States. *Weather Forecast.* **20**: 577–595.
- Doswell CA III, Brooks HE, Dotzek N. 2009. On the implementation of the Enhanced Fujita Scale in the USA. *Atmos. Res.* **93**: 554–563.
- Edwards R, LaDue J, Ferree J, Scharfenberg K, Maier C, Coulbourne L. 2013. Tornado intensity estimation: past, present, and future. *Bull. Am. Meteorol. Soc.* **94**(5): 641–653.
- Efron B, Tibshirani R. 1994. *An Introduction to the Bootstrap*. CRC Press: Boca Raton, FL.
- Farney T, Dixon P. 2014. Variability of tornado climatology across the continental United States. *Int. J. Climatol.* **35**(10): 2993–3006.
- Gensini V, Mote T. 2014. Estimations of hazardous convective weather in the United States using dynamical downscaling. *J. Clim.* **27**: 6581–6598.
- Gensini V, Mote T. 2015. Downscaled estimates of late 21st century severe weather from CCSM3. *Clim. Change* **129**: 307–321.
- Grazulis T. 1993. *Significant Tornadoes, 1680–1991*. Environmental Films: St. Johnsbury, VT; 1326 pp.
- Huggel C, Stone D, Auffhammer M, Hansen G. 2013. Loss and damage attribution. *Nat. Clim. Change* **3**: 694–696.
- IPCC. 2014. Climate change 2014: mitigation of climate change. Contribution of Working Group III to the Fifth Assessment. Report of the Intergovernmental Panel on Climate Change. IPCC. <http://www.ipcc.ch/report/ar5/syr/> (accessed 1 June 2015)
- Karstens C, Stumpf G, Ling C, Hua L, Kingfield D, Smith T, et al. 2015. Evaluation of a probabilistic forecasting methodology for severe convective weather in the 2014 hazardous weather testbed. *Weather Forecast.* **3**: 1551–1570, DOI: 10.1175/WAF-D-14-00163.1.

- Kunkel K, Karl T, Brooks H, Kossin J, Lawrimore J, Arndt D, et al. 2013. Monitoring and understanding trends in extreme storms: state of knowledge. *Bull. Am. Meteorol. Soc.* **94**(4): 499–514.
- Maloney M, Preston B. 2014. A geospatial dataset for U.S. hurricane storm surge and sea-level rise vulnerability: development and case study applications. *Clim. Risk Manage.* **2**: 26–41.
- Mann M, Berck P, Moritz M, Battlori E, Baldwin J, Gately C, et al. 2014. Modeling residential development in California from 2000 to 2050: integrating wildfire risk, wildland and agricultural encroachment. *Land Use Policy* **41**: 438–452.
- Meyer C, Brooks H, Kay M. 2002. A hazard model for tornado occurrence in the United States. Extended Abstracts, In *American Meteorological Society 13th Symposium on Global Change and Climate Variations*, January 13–17, Orlando, FL.
- Mooney C. 1997. *Monte Carlo Simulation*, Vol. 116. Sage Publications: Thousand Oaks, CA.
- Morss R, Wilhelmi O, Meehl G, Dilling L. 2011. Improving societal outcomes of extreme weather in a changing climate: an integrated perspective. *Ann. Rev. Environ. Resour.* **36**: 1–25.
- Nicholls RJ, Small C. 2002. Improved estimates of coastal population and exposure to hazards released. *Eos Trans. AGU* **83**: 301–305.
- Patterson L, Doyle M. 2009. Assessing effectiveness of national flood policy through spatiotemporal monitoring of socioeconomic exposure. *J. Am. Water Resour. Assoc.* **45**: 237–252.
- Pelletier J, Murray B, Pierce J, Bierman P, Breshears D, Crosby B, et al. 2015. Forecasting the response of Earth's surface to future climatic and land-use changes: a review of methods and research needs. *Earth's Future* **3**: 220–251.
- Petersen A. 2012. *Simulating Nature: A Philosophical Study of Computer-Simulation Uncertainties and Their Role in Climate Science and Policy Advice*. CRC Press: London, UK.
- Pielke R Jr. 2005. Attribution of disaster losses. *Science* **311**: 1615–1616.
- Pielke R Jr, Gratz J, Landsea C, Collins D, Saunders M, Musulin R. 2008. Normalized hurricane damage in the United States: 1900–2005. *Nat. Hazards Rev.* **9**: 29–42.
- Prevatt D, van de Lindt J, Back E, Graettinger A, Pei S, Coulbourne W, et al. 2012. Making the case for improved structural design: tornado outbreaks of 2011. *Leadership Manage. Eng.* **12**: 254–270.
- Rae S, Stefkovich J. 2000. The tornado damage risk assessment predicting the impact of a big outbreak in Dallas–Fort Worth, Texas. Extended Abstracts. In *20th Conference on Severe Local Storms*. American Meteorological Society, Orlando, FL.
- Rahman A, Weinmann P, Hoang T, Laurenson E. 2002. Monte Carlo simulation of flood frequency curves from rainfall. *J. Hydrol.* **256**(3): 196–210.
- Rosencrants T, Ashley W. 2015. Spatiotemporal analysis of tornado exposure in five U.S. metropolitan areas. *Nat. Hazards* **78**: 121–140.
- Schlossberg M. 2003. GIS, the US Census and neighbourhood scale analysis. *Plan. Practice Res.* **18**: 213–217.
- SEDAC. 2015. U.S. Census grids. Socioeconomic Data and Applications Center, Columbia University. <http://sedac.ciesin.columbia.edu/usgrid/> (accessed 15 June 2015)
- Simmons K, Kovacs P, Kopp G. 2015. Tornado damage mitigation: benefit/cost analysis of enhanced building codes in Oklahoma. *Weather Clim. Soc.* **7**: 169–178, DOI: 10.1175/WCAS-D-14-00032.1.
- Simmons K, Sutter D. 2007. Tornado shelters and the housing market. *Constr. Manage. Econ.* **25**: 1119–1126.
- Smith B, Dean A, Thompson R, Leitman, E, Grams, J. 2015b. Developmental work at the Storm Prediction Center in pursuit of tornadic supercell probability and tornado Intensity estimation using a severe supercell dataset. In *2015 NWA Meeting*, 17–22 October 2015, Oklahoma City, OK.
- Smith A, Katz R. 2013. US billion-dollar weather and climate disasters: data sources, trends, accuracy and biases. *Nat. Hazards* **7**(2): 387–410.
- Smith B, Thompson R, Dean A, Marsh P. 2015a. Diagnosing the conditional probability of tornado damage rating using environmental and radar attributes. *Weather Forecast.* **30**: 914–932.
- Smith B, Thompson R, Grams J, Broyles C, Brooks H. 2012. Convective modes for significant severe thunderstorms in the contiguous United States. Part I: storm classification and climatology. *Weather Forecast.* **27**(5): 1114–1135.
- Strader S, Ashley W. 2015. The expanding bull's eye effect. *Weatherwise* **68**(5): 23–29.
- Strader S, Ashley W, Irizarry A, Hall S. 2015a. A climatology of tornado intensity assessments. *Meteorol. Appl.* **22**: 1365–1392.
- Strader S, Ashley W, Walker J. 2015b. Changes in volcanic hazard exposure in the Northwest USA from 1940 to 2100. *Nat. Hazards* **77**: 1365–1392.
- Suckling P, Ashley W. 2006. Spatial and temporal characteristics of tornado path direction. *Prof. Geogr.* **58**: 20–38.
- Theobald D. 2005. Landscape patterns of exurban growth in the USA from 1980 to 2020. *Ecol. Soc.* **10**(32). <http://www.tetonwyo.org/complan/LDRUpdate/RuralAreas/Additional%20Resources/Theobald2005.pdf> (accessed 2 February 2015)
- Thorne P, Vose R. 2010. Reanalysis suitable for characterizing long-term trends: are they really achievable? *Bull. Am. Meteorol. Soc.* **91**: 353–361.
- Tippett M, Allen J, Gensini V, Brooks H. 2015. Climate and hazardous convective weather. *Curr. Clim. Change Rep.* **1**(2): 60–73.
- Trapp R, Diffenbaugh N, Brooks H, Baldwin M, Robinson E, Pal J. 2007. Changes in severe thunderstorm environment frequency during the 21st century caused by anthropogenically enhanced global radiative forcing. *Proc. Natl. Acad. Sci. U. S. A.* **104**: 19719–19723.
- Trapp R, Robinson E, Baldwin M, Diffenbaugh N, Schwedler B. 2011. Regional climate of hazardous convective weather through high-resolution dynamical downscaling. *Clim. Dyn.* **37**: 677–688.
- Twisdale L, Dunn W, Davis T, Horie Y. 1981. Tornado missile simulation and design methodology. EPRI NP-2005, EPRI: Palo Alto, CA.
- Van de Walle B, Turoff M. 2007. Emergency response information systems: emerging trends and technologies. *Commun. ACM* **50**(3): 29–31.
- Verbout S, Brooks H, Leslie L, Schultz D. 2006. Evolution of the U.S. Tornado database: 1954–2003. *Weather Forecast.* **21**: 86–93.
- Weisstein E. 2002a. Sphere point picking. *MathWorld* – a Wolfram web resource. <http://mathworld.wolfram.com/SpherePointPicking.html> (accessed 21 May 2015).
- Weisstein E. 2002b. Random walk – 1-dimensional. *MathWorld* – a Wolfram web resource. <http://mathworld.wolfram.com/RandomWalk1-Dimensional.html> (accessed 21 May 2015).
- Wilby R. 2007. A review of climate change impacts on the built environment. *Built Environ.* **33**(1): 31–45.
- Wurman J, Robinson P, Alexander C, Richardson Y. 2007. Low-level winds in tornadoes and potential catastrophic tornado impacts in urban areas. *Bull. Am. Meteorol. Soc.* **88**(1): 31–46.